sciendo

ADVANCED RESEARCH IN LIFE SCIENCES
8, 2024, 1 – 14

www.degruyter.com/view/j/arls

DOI: 10.2478/arls-2024-0001
Research Article

Exploring the Anti-Inflammatory Potential of Phytochemicals from *Anvillea radiata*: *In Vitro* Assay, Molecular Docking, and Molecular Dynamics Simulations

Amal Belakredar[1], Farouk Boudou[2], Sehmi Abdelghani[3]

[1]*Department of Environmental Sciences, Faculty of Nature and Life Sciences, Djillali LIABES University Sidi-Bel-Abbès, BP 89, 22000 Sidi-Bel-Abbès - Algeria.*
[2]*Department of Biology, Faculty of Sciences, Djillali LIABES University Sidi-Bel-Abbès, BP 89, 22000 Sidi-Bel-Abbès – Algeria.*
[3]*Department of Natural and Life Sciences, Faculty of Sciences and Technology, University of Tissemsilt, 38000 Tissemsilt, Algeria*

Received October, 2023; Revised December, 2023; Accepted December, 2023

Abstract
This study delves into the comprehensive evaluation of phytochemicals extracted from Anvillea radiata, with a focus on their potential anti-inflammatory applications. High-performance liquid Chromatography analysis reveals the dominance of catechin in the aqueous extract, alongside other compounds such as syringic acid, 3,4-dihydroxybenzoic acid, and vanillic acid, as well as quercetin-3-β-D-glucoside and rutin in smaller quantities. An in vitro anti-inflammatory assay demonstrates the superior effectiveness of *A. radiata* aqueous extract at lower concentrations compared to Aspirin, raising possibilities for reduced side effects and enhanced cost-effectiveness. Drug-likeness predictions emphasize the potential of catechin, syringic acid, and vanillic acid for drug development due to their molecular characteristics. Toxicity risk assessment indicates that catechin, quercetin-3-β-D-glucoside, and rutin exhibit low toxicity risks and favorable drug-likeness properties. Molecular docking analysis highlights promising interactions between the identified compounds and crucial anti-inflammatory (COX-2, MPO, IL1β, IL6, and TNFα.) target proteins. Notably, catechin demonstrates a strong binding affinity to these proteins. Molecular dynamics simulations further support catechin's potential, revealing significant deformability in complexes with COX-2 and MPO, indicating high structural flexibility. The variance map shows higher cumulative variances and the elastic network map yields satisfactory outcomes, further reinforcing the potential of *A. radiata* aqueous extract compounds, with catechin as a standout candidate for anti-inflammatory drug development.

Keywords: *Anvillea radiata*, Catechin, Anti-inflammatory, Molecular docking, Molecular dynamic.

Introduction

Inflammation is a complex physiological response that plays a crucial role in the body's defense mechanism against infection and injury [1]. While acute inflammation is a natural and essential process, chronic inflammation can lead to a host of diseases such as rheumatoid arthritis, cardiovascular disorders, and inflammatory bowel disease (IBD) [2]. A select group of proteins emerges as pivotal conductors, orchestrating the symphony of immune responses and inflammation. Among these key players are COX-2 (Cyclooxygenase-2), MPO (Myeloperoxidase), IL-1β (Interleukin-1β), IL-6 (Interleukin-6), and TNF-α (Tumor Necrosis Factor-alpha), each holding crucial roles in shaping health and disease outcomes [3-5]. COX-2, an enzyme catalyzing the synthesis of proinflammatory prostaglandins, plays a central part in pain and inflammation modulation [6]. MPO, a key player in

* Corresponding author: **F. Boudou, Email:** farouk.boudou@univ-saida.dz
© 2024 F. Boudou et al., published by De Gruyter Open.
This work was licensed under the Creative Commons Attribution-NonCommercial-NoDerivs 3.0 License

innate immunity, exerts its antimicrobial activity through the generation of reactive oxygen species [7]. IL-1β, a potent proinflammatory cytokine, initiates and amplifies immune responses, albeit its uncontrolled expression is implicated in autoimmune disorders [8]. IL-6, a multifunctional cytokine, influences a wide range of processes including acute-phase responses and adaptive immunity regulation [9]. TNF-α, a master regulator of inflammation, is implicated in various inflammatory diseases [10], and its targeted therapy has revolutionized treatment approaches [11]. However, to mitigate excessive inflammation and alleviate associated symptoms, anti-inflammatory drugs, such as nonsteroidal anti-inflammatory drugs (NSAIDs) and corticosteroids, have been widely prescribed [12, 13]. However, the use of synthetic anti-inflammatory drugs is not without its drawbacks [14]. NSAIDs, in particular, are known to cause adverse effects like gastrointestinal bleeding, ulcers, and an increased risk of cardiovascular events [15, 16]. Long-term use of corticosteroids can also lead to numerous side effects, including osteoporosis, weight gain, and immune system suppression [17]. The mounting concerns over the safety of conventional anti-inflammatory medications have led to an urgent quest for safer and more natural alternatives [18]. In recent years, there has been a growing interest in traditional medicine and the use of natural plant extracts as a source of potential anti-inflammatory agents [19]. Indigenous medicinal plants have been used for centuries in various cultures to treat inflammatory conditions [20]. One region that stands out for its rich botanical diversity is Algeria, known for its numerous endemic plant species with unique therapeutic properties [21]. Among the promising Algerian endemic plants is *Anvillea radiata* (Coss and Dur), commonly known as "Nogd", which has been traditionally used by the local Berber population for its medicinal properties [22]. Studies have indicated that *A. radiata* possesses potent anti-inflammatory effects due to its rich phytochemical composition, including flavonoids, terpenoids, and phenolic compounds [23]. These natural compounds have demonstrated the ability to inhibit key pro-inflammatory mediators, such as cytokines and prostaglandins, thus reducing inflammation and its associated symptoms [24]. By exploring the potential of Algerian endemic plants like *A. radiata* as natural anti-inflammatory alternatives, we aim to shed light on the remarkable therapeutic potential that traditional medicine has to offer. The aim of this study is to investigate the anti-inflammatory potential of plant extracts obtained through decoction, identify natural polyphenols using High-Performance Liquid Chromatography (HPLC), and assess their in vitro anti-inflammatory activity through protein denaturation assay. Additionally, the study aims to conduct in silico analysis, including drug-likeness prediction, molecular docking and molecular dynamic against five crucial inflammatory molecular targets, namely COX-2 (PDB ID: 4COX), MPO (PDB ID: 3ZS0), IL1β (PDBID: 1T4Q), IL6 (PDBID: 1P9M), and TNFα (PDBID: 2AZ5).

Materials and methods

Plant Material and Extraction

The aerial part of the native Algerian plant Anvillea radiate obtained from an herbalist located in the town of Tamarsset, the southernmost region of Algeria (latitude: 22.7869, longitude: 5.52722), was used. The aqueous extract of A. radiate (AAE) was prepared using the decoction method described by [25]. The plant material was thoroughly washed, dried, and powdered. A 10 g portion of the powder was then boiled in 100 mL of water at 100°C using a water bath reflux system for 15 minutes. The mixture was filtered through Whatman Millipore N°1 filter paper to remove any solid particles. The filtrate obtained was combined and centrifuged at 4000 rpm for 20 minutes. The supernatant was then concentrated to dryness using a rotary evaporator, and the residue obtained was stored at 4°C until use.

Phytocompounds identification by High-performance liquid chromatography (HPLC)

To identify the phytochemicals in *Anvillea radiata,* the AAE extract was reconstituted, filtered through a 0.45 mm membrane filter, and analyzed using an Agilent Series 1100 HPLC Chromatograph coupled with a multiwavelength detector (UV/Visible spectrum). The separation process utilized a Kinetex column (Phenomenex, Torrance, CA, 100 4.6mmI.D. with 2.6 m particle size). The mobile phase consisted of a 0.1 percent formic acid aqueous solution and methanol (MeOH). The elution of compounds occurred over 15 minutes with a linear gradient from 5% to 95% MeOH. Peaks were monitored at 280 nm. Polyphenolic compounds were identified based on their retention times and spectral characteristics compared to standard peaks.

Protein Denaturation Inhibition Assay

The AAE extract's anti-inflammatory activity was evaluated using the in vitro albumin denaturation inhibition assay. To assess the ability of the extracts to inhibit albumin denaturation, following the modified method of Nagavekar and Singhal, (2018) [26]. As a reference, Aspirin (acetylsalicylic acid - ASA), a standard anti-inflammatory drug, was used. The reaction mixture consisted of 1 mL of 1% bovine serum albumin (BSA), 1 mL of

phosphate-buffered saline (PBS, pH 6.8), and 0.2 mL of the standard drug or extract. The control contained only the solvent in a similar volume. The mixture was thoroughly mixed and heated at 70 °C for 5 minutes. After cooling, the absorbance was measured at 660 nm using a UV-VIS spectrophotometer. The percentage inhibition of protein denaturation was calculated using the formula:

$$I\ \% = (A1 - A2/A1) \times 100$$

where A1 represents the absorbance of the control, and A2 represents the absorbance of the test or drug.

Drug-likeness prediction

The drug-likeness properties of the AAE's identified phytochemicals were investigated using the SwissADME web database (http://www.swissadme.ch/index.php). The respective SMILES notations of compounds were obtained from the PubChem database (www.pubchem.ncbi.nlm.nih.gov), or they were converted into molecular sketchers based on ChemAxon's Marvin JS. Subsequently, the physicochemical and pharmacokinetic properties were assessed to determine compliance with Lipinski's Rule of Five [27], and Ghose filter [28]. Lipinski's Rule of Five states that an orally active drug typically has no more than one violation of the following criteria: no more than 5 H-bond donors, 10 H-bond acceptors, a molecular weight (MW) less than 500, and an octanol-water partition coefficient (log P) not exceeding 5 (or MlogP > 4.15). On the other hand, the Ghose filter, an extension of Lipinski's rule, includes a Log P partition coefficient ranging from -0.4 to +5.6, molar refraction between 40 and 130, molecular weight between 180 and 480, and several atoms between 20 and 70 (including H-bond donors and acceptors).

Toxicity risks assessment

The primary focus in searching for lead compounds in pharmacology is assessing their potential for toxicity, which can be predicted using computational methods like the OSIRIS property exploration tool [29]. This study specifically examined natural compounds for mutagenic, tumorigenic, irritant, and reproductive toxicity. OSIRIS Property Explorer validates chemical structures and rapidly computes various drug-related properties. These predictions are recorded and color-coded, where red signifies high-risk properties, while green indicates properties suitable for drug usage [30].

Molecular docking study

For the present study, Autodock, running on PyRx-Python 0.8 software [31], was used to perform the calculations. Crystal structures of five inflammatory molecular targets, namely COX-2 (PDB ID: 4COX), MPO (PDB ID: 3ZS0), IL1β (PDB ID: 1T4Q), IL6 (PDB ID: 19PM), and TNFα (PDB ID: 2AZ5), were extracted from the Protein Data Bank (PDB) at www.rcsb.org. Enzyme preparation was performed using Molegro 2.5 software. The 3D structures of the ligands identified by HPLC in the AAE extract were retrieved from the PubChem database (www.pubchem.ncbi.nlm.nih.gov). To enable docking, a grid map representing protein binding sites was generated using AutoGrid. The CASTp (Computer Atlas Surface Topology of Protein) server was utilized to identify and confirm the active regions of the examined proteins (COX-2, MPO, IL1β, IL6, and TNFα). This server employs accurate computer geometry techniques to assess protein pockets and voids [32]. The CASTp server employs a default measurement of 1.4 Angstroms, and it only accepts values within the range of 0.0 to 10.0 Angstroms [33]. Finally, Receptor-ligand interaction options were applied in molecular docking studies using BIOVIA Discovery Studio Visualizer 2021 and LigPlot+ v.2.

Molecular dynamics simulation

To assess the stability and movement of the protein-ligand complexes, the docking structures with the lowest docking energy, and the best pharmacological and toxicological characteristics were subjected to molecular dynamics simulations. These simulations were carried out using the iMODS server, which can be accessed at http://imods.chaconlab.org [34]. The iMODS server plays a crucial role in exploring different modes of motion and generating potential transition pathways between structurally similar proteins. One of the functions of the iMODS server is to evaluate protein stability, which it accomplishes by calculating the internal coordinates of the protein through normal mode analysis (NMA). The server represents protein stability using various parameters, including a main-chain deformability plot, B-factor values, eigenvalues, covariance matrix, and an elastic network model.

Results and discussion

HPLC Identification of phytochemical compounds

Table 1 presents the results of the HPLC analysis of the AAE aqueous extract, giving an overview of the composition of this extract. Notably, the predominant compound detected is catechin, accounting for 4.917% of the extract, followed by the presence of syringic acid, 3,4-dihydroxybenzoic acid, vanillic acid, quercetin-3-β-D-glucoside, and rutin, albeit in lesser proportions.

The focus on catechin underlines its role as the main bioactive constituent of the extract and indicates the potential importance of this compound for AAE. These results not only highlight the need to further explore the potential health benefits of AAE but also suggest the existence of potential synergistic effects between the compounds identified. Catechin is well known for its potent antioxidant and anti-inflammatory properties, making it central to the medicinal value attributed to many Asteraceae species, including *A. radiata* [35]. The diversity of phytochemical composition revealed by this analysis gives us a better understanding of the therapeutic potential of AAE and underlines the interest in exploring its biological activities.

Table1. HPLC data for aqueous extract of *Anvillea radiata*

Identified compound	Retention time (min)	Proportion (%)
Catechin	6.653	4.917
Syringic acid	7.347	0.052
3,4-Dihydroxybenzoic acid	8.229	0.565
Vanillic acid	8.525	0.224
Quercetin-3-β-D-glucoside	8.956	0.166
Rutin	9.127	0.071

In vitro anti-inflammatory assay

The data presented in Fig. 1 shows that Aspirin (ASA) and *A. radiata* aqueous extract (AAE) have varying degrees of inhibition on protein denaturation depending on the concentration. ASA exhibits higher inhibition at 1 mg/mL and 0.5 mg/mL, while AAE surpasses ASA at lower concentrations of 0.25 mg/mL, 0.125 mg/mL, and notably at 0.0313 mg/mL. This suggests that AAE may be more effective at lower dosages, potentially leading to reduced side effects and improved cost-effectiveness. Furthermore, the natural origin of AAE from A. radiata makes it an appealing candidate with potentially fewer adverse effects compared to synthetic drugs like ASA. However, in silico research is needed to understand the underlying mechanisms of AAE's inhibitory action and explore its potential as an alternative to ASA in protein denaturation inhibition and biomedical applications. Indeed, the mechanism by which AAE inhibits protein denaturation is still poorly understood. However, a study conducted by Chen et al. (2022) [36] highlighted the impact of certain phenolic compounds (tannic acid, epigallocatechin gallate, quercetin, quercitrin) on casein. These compounds led to aggregation, increased emulsifying, and foaming stability, and induced changes in casein structure. Molecular interactions were observed between phenolic compounds and casein, with their structural characteristics, including molecular weight, hydroxyl group location, acylation, and glycosylation, playing a central role in influencing these interactions. In the same order, suggests that interaction with tannins protects protein structure from temperature-induced damage. This protective effect could be due to the establishment of a chemical bond between the tannin and the protein that cross-links the molecule to decrease the entropy of the polypeptide, which could corroborate the decrease in the rate of denaturation.

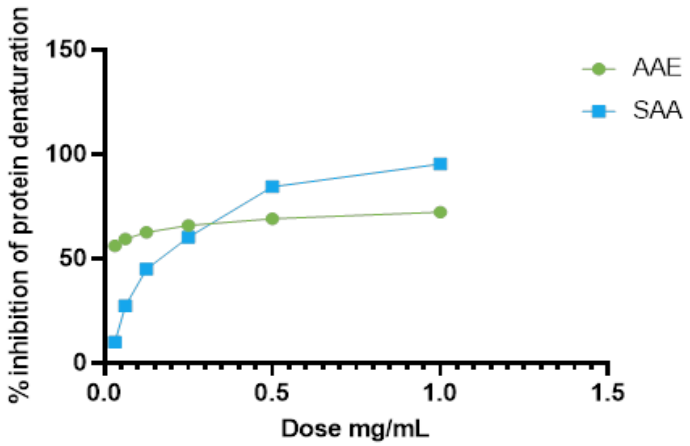


Figure 1. Percentage of protein denaturation inhibition by *A. radiata* aqueous extract (AAE) and Aspirin (ASA)

Drug-likeness prediction

Table 2 provides drug-likeness predictions for the identified compounds using SwissADME, offering valuable insights into their molecular properties and adherence to key drug development rules. The data reveals that catechin, syringic acid, vanillic acid, and quercetin-3-β-D-glucoside largely satisfy Lipinski's rule of five, a standard for predicting drug-likeness. This indicates that these compounds possess favorable molecular characteristics for potential drug development. However, quercetin-3-β-D-glucoside and rutin violate Ghose's filter, suggesting some deviation from the optimal range of parameters for drug-likeness, specifically related to lipophilicity and molecular size. This information suggests that catechin, syringic acid, and vanillic acid have better drug-like properties and are more likely to be considered for further development based on their molecular features.

Table 2. Drug-likeness prediction of identified compounds using SwissADME

Ligand	Molecular weight (MW) (g/mol)	Num. H-bond acceptors (Hba)	Num. H-bond donors (Hbd)	Molar Refractivity (MR)	MLOGP	WLOGP	Lipinski rule	Ghose filter
Catechin_CID_73160	290.27	6	5	74.33	1.22	0.24	Yes; 0 violation	Yes
Syringic acid_CID_10742	198.17	5	2	48.41	0.49	1.11	Yes; 0 violation	Yes
3,4-Dihydroxybenzoic acid_CID_72	154.12	4	3	37.45	0.40	0.80	Yes; 0 violation	No; 3 violations: MW<160, MR<40, #atoms<20
Vanillic acid_CID_8468	168.15	4	2	41.92	0.74	1.10	Yes; 0 violation	Yes
Quercetin-3-β-D-glucoside_CID_44259136	464.38	12	8	110.16	-2.59	-0.54	No; 2 violations: NorO>10, NHorOH>5	No; 1 violation: WLOGP<-0.4
Rutin_CID_5280805	610.52	16	10	141.38	-3.89	-1.69	No; 3 violations: MW>500, NorO>10, NHorOH>5	No; 4 violations: MW>480, WLOGP<-0.4, MR>130, #atoms>70

Toxicity risk assessment

Table 3 evaluates the toxicity risk, drug score, and drug-likeness of the identified compounds using OSIRIS property explorer. Among the compounds, catechin, quercetin-3-β-D-glucoside, and rutin exhibit favorable drug-likeness, indicating their potential suitability for drug development. These compounds have green indications across various properties, suggesting a lower risk of harmful effects. Rutin, in particular, stands out with a high drug score of 3.31, indicating a promising candidate. On the other hand, syringic acid and vanillic acid display some red indications in the mutagenic property, signaling a moderate risk in this aspect.

Table 3. Toxicity risk, drug score, and drug-likeness of identified compounds predicted by OSIRIS property explorer

Ligand	Mutagenic	Tumorigenic	Irritant	Reproductive effective	Drug-likeness	Drug-score
Catechin_CID_73160	Green	Green	Green	Green	1.92	0.87
Syringic acid_CID_10742	Red	Green	Green	Green	1.99	0.44
3,4-Dihydroxybenzoic acid_CID_72	Red	Green	Green	Green	-1.12	0.43
Vanillic acid_CID_8468	Red	Green	Green	Green	-1.31	0.35
Quercetin-3-β-D-glucoside_CID_44259136	Green	Green	Green	Green	-2.17	0.43
Rutin_CID_5280805	Green	Green	Green	Green	3.31	0.57

The outcomes are presented as a color and value. Red and green colors indicate a property with a high risk of harmful effects and drug confirmation behavior, respectively.

Molecular docking analysis

The CASTp server using precise computational geometry techniques to assess protein pockets and voids was used to identify and confirm the active regions of the proteins examined (COX-2, MPO, IL1β, IL6, and TNFα). The active site regions of the target proteins are shown in Fig. 2. The data in Table 4 provides valuable information about the binding affinity and molecular interactions of the identified compounds with target proteins associated with anti-inflammatory activity. This data suggests potential interactions of the compounds with COX-2, MPO, IL1β, IL6, and TNFα, implying their involvement in these pathways and potential therapeutic effects. This insight further underscores the importance of the identified compounds in *A. radiata* as potential candidates for further research in drug development and the understanding of their mechanisms of action. Among the compounds studied, only catechin meets the criteria for drug-likeness and toxicity safety, suggesting it is a promising candidate for further drug development. The binding affinity and molecular interaction data in Table 4 reveal important insights into the potential mechanisms of action of these compounds, especially concerning their anti-inflammatory and antioxidant activities. Catechin shows a strong binding affinity to multiple target proteins associated with anti-inflammatory and antioxidant effects. For example, it exhibits a high binding affinity to COX-2 (Fig. 3-A), a key enzyme involved in inflammation, and MPO, an enzyme implicated in oxidative stress (Fig. 3-B). These interactions indicate that catechin might have significant anti-inflammatory and antioxidant properties, making it a potentially valuable compound for drug development in this context.

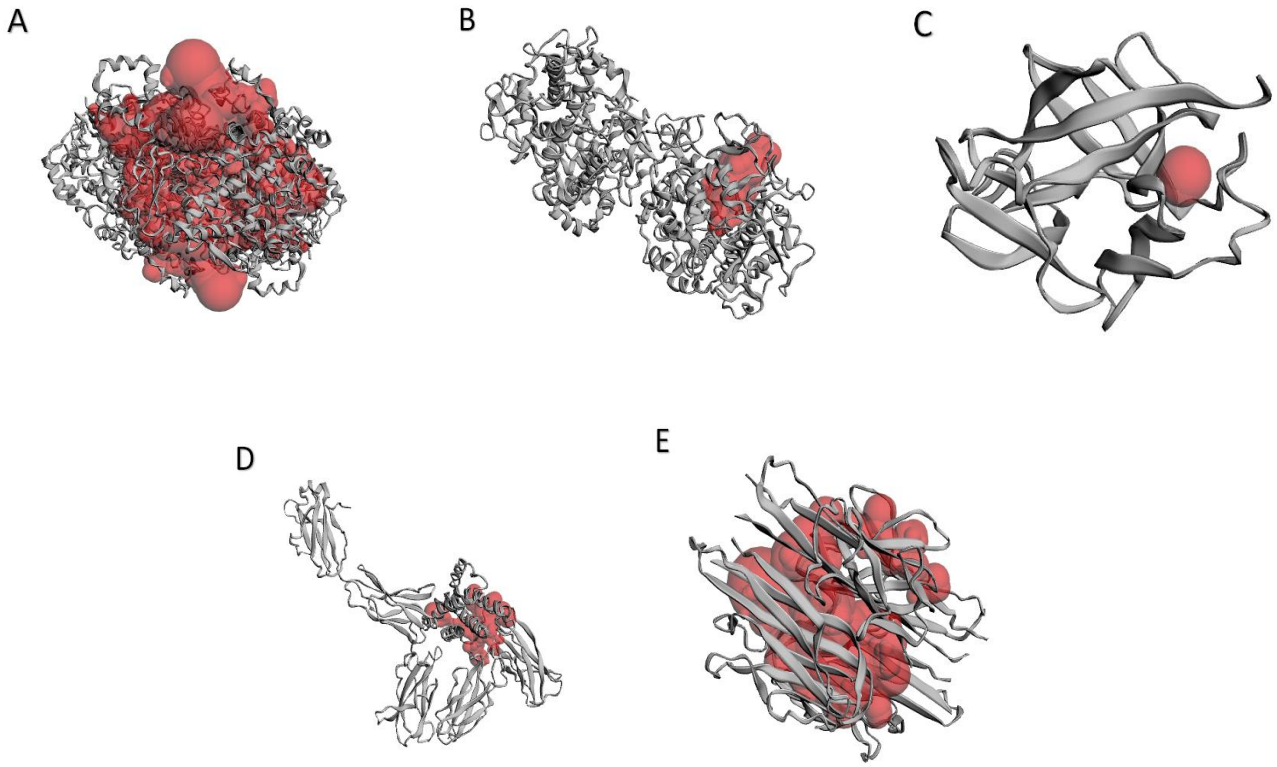


Figure 2. Confirmation of active pocket sites from CASTp software for the target proteins. COX-2 (A), MPO (B), IL1β (C), IL6 (D), and TNFα (E).

Table 4. Binding affinity and molecular interactions of the ligands studied and standard drugs with target proteins for anti-inflammatory and antioxidant activities

Targets (PDB ID)	Ligands (PubChem ID)	Binding affinity Kcal/mol	Hydrogen bonding (chain)	Hydrophobic interactions (chain)
COX-2 (PDB ID: 4COX)	Catechin_CID_73160	-9.3	Cys47(A), Ser49(B), Gln327(B), Ala156(A), Asn39(A), Gln461(A)	Pro154(A), Pro153(A), Gly135(A), Tyr136(A), Met48(A), Cys159(A), Cys36(A), Cys159(A), Cys37(A), Val155(A)
	Syringic acid_CID_10742	-6.2	Arg44(D), Gln461(D), Asn39(D), Arg44(D)	Tyr130(D), Pro153(D), Leu152(D), Gly45(D), Glu465(D)
	3,4-Dihydroxybenzoic acid_CID_72	-6.5	Met522(B), Ser530(B), Tyr385(B)	Leu352(B), Phe518(B), Gly526(B), Trp387(B), Leu384(B)
	Vanillic acid_CID_8468	-6.5	Trp387(B), Thr206(B)	Ala202(B), Tyr385(B), His207(B), His388(B), Gln203(B), Leu390(B), Ala199(B), Leu391(B)
	Quercetin-3-β-D-glucoside_CID_44259136	-10.3	Gln461(B), Gly135(B), Cys36(B), Arg44(B), Ala151(B), Glu465(B)	Arg469(B), Lys468(B), Cys41(B), Asn39(B), Cys47(B), Pro153(B), Glu46(B), Tyr130(B), Gly45(B), Leu152(B)
	Rutin_CID_5280805	-11.5	Tyr136(D), Asn34(D), Gln461(D), Asn39(D), Pro154(D), Ala156(D), Ser49(D), Gln327(C)	Gly324(C), Trp323(C), Pro35(D), Ala33(D), Asp158(D), Glu322(C), Cys159(D), Val155(D), Cys37(D), Cys36(D), Met48(D)
MPO (PDB ID: 3ZS0)	Catechin_CID_73160	-9.2	Tyr296(C), Met87(A), Arg333(C), Thr329(C)	Gly335(C), Gln91(A), His95(A), His336(C), Arg239(C), Gly90(A), Phe332(C), Asp94(A), Tyr334(C)
	Syringic acid_CID_10742	-6.3	/	Met87(A), His336(C), Ile339(C), Gln91(A), Tyr296(C), Asp94(A), Arg333(C), Phe332(C), Tyr334(C), Gly90(A), Gly335(C)
	3,4-Dihydroxybenzoic acid_CID_72	-7.6	Arg8(A), Lys282(C)	Gly285(C), Phe512, Tyr7(A), Tyr7(A), Arg281(C), Ala286(C)

	Vanillic acid_CID_8468	-6.4	His336(C)	Met87(A), Gln91(A), Gly335(C), Asp94(A), Tyr334(C), Tyr296(C), Phe332(C), Gly90(A)
	Quercetin-3-β-D-glucoside_CID_44259136	-9.2	Glu102(B), Arg424(D), Asp94(B), Asp98(B), Thr100(B),	Leu420(D), Arg239(D), Arg333(D), Gln91(B), His336(D), Leu406(D), Glu242(D), Leu417(D)
	Rutin_CID_5280805	-11.0	Met87(A), Arg239(C), Glu102(A), Arg333(C), Asp98(A), Thr329(C), Asp94(A),	Gly335(C), His95(A), His336(C), Phe407(C), Leu417(C), Arg424(C), Gln91(A), Phe332(C)
IL1β (PDBID: 1T4Q)	Catechin_CID_73160	-6.4	Leu62(A), Ser43(A), Ser153(A), Glu64(A), Lys65(A)	Gly61(A), Ser5(A), Asn7(A), Lys63(A), Tyr68(A), Asn66(A)
	Syringic acid_CID_10742	-5.0	Thr144(A), Gly139(A), Gln126(A), Gln14(A), Ser13(A)	Asp142(A), Ile143(A), Gly140(A), Asp145(A)
	3,4-Dihydroxybenzoic acid_CID_72	-5.0	Pro87(A), Glu64(A)	Tyr90(A), Ser43(A), Lys63(A), Tyr68(A), Lys65(A), Leu62(A)
	Vanillic acid_CID_8468	-5.0	Lys63(A), Gln39(A),	Leu62(A), Val40(A), Met20(A), Gln38(A), Val41(A)
	Quercetin-3-β-D-glucoside_CID_44259136	-7.2	Pro87(A), Val3(A), Asn7(A), Ser43(A), Ser5(A), Leu62(A), Glu64(A), Lys65(A)	Pro91(A), Leu6(A), Lys63(A), Asn66(A), Tyr90(A
	Rutin_CID_5280805	-7.2	Lys65(A), Tyr68(A), Ser43(A), Asn7(A), Ser153(A), Ser5(A), Tyr90(A), Pro87(A)	Asn66(A), Lys63(A), Arg4(A), Ala1(A), Val3(A), Pro2(A), Pro91(A)
IL6 (PDBID: 1P9M)	Catechin_CID_73160	-7.9	Arg128(A), Glu129(A), Phe136(A), Ala152(A), Thr130(A)	Pro157(A), Asn135(A), Arg154(A), Thr134(A), Gly127(A)
	Syringic acid_CID_10742	-5.3	/	Leu92(B), Pro139(B), Glu93(B), Thr138(B), Val96(B), Asn144(B), Glu95(B)

	3,4-Dihydroxybenzoic acid_CID_72	-5.6	Thr125(C), Glu96(C), Ser177(C)	Pro121(C), Val179(C), Gly180(C), Lys182(C), Val175(C), Ser181(C)
	Vanillic acid_CID_8468	-5.4	Arg233(C), Glu278(C), Ser229(A), Asp34(B)	Phe279(C), Leu33(B), Arg30(B)
	Quercetin-3-β-D-glucoside_CID_44259136	-7.6	Ala152(A), Phe136(A), Arg154(A), Arg128(A), Gly127(A), Thr130(A)	Asn135(A), Pro157(A), Glu129(A), Thr134(A)
	Rutin_CID_5280805	-8.9	Ser229(A), Ser37(B), Thr258(A), Asp34(B)	Leu33(B), Phe279(C), Trp249(C), Met250(C), Lys228(A), Lys252(C), Arg233(C), Arg30(B), Ile232(A)
TNFα (PDBID: 2AZ5)	Catechin_CID_73160	-8.6	Gln125(D), Gln125(B),	Phe124(D), Leu93(B), Asn92(B), Arg82(D),Val91(D), Val91(B), Arg82(B), Leu93(D), Asn92(D), Phe124(B)
	Syringic acid_CID_10742	-5.8	Ser60(B), Tyr151(B),	Leu57(A), Tyr59(B), Gln61(B), Tyr119(B), Tyr119(A), Leu120(A), Tyr59(A), Gly121(A), Gly122(A)
	3,4-Dihydroxybenzoic acid_CID_72	-5.6	Gln125(D), Leu93(B)	Phe124(D), Phe124(B), Leu93(D), Val91(D), Val91(B), Arg82(D)
	Vanillic acid_CID_8468	-5.6	Ser60(B), Tyr151(B)	Tyr59(A), Gly121(A), Leu57(A), Tyr59(B), Gly122(A), Gln61(B), Tyr119(B), Leu120(A)
	Quercetin-3-β-D-glucoside_CID_44259136	-8.6	Gln125(D), Glu127(D), Tyr87(D), Arg82(D)	Leu126(D), Asn92(B), Phe124(B), Leu93(B), Leu93(D), Thr89(D), Val91(D)
	Rutin_CID_5280805	-9.0	Tyr151(A), Gly121(A), Ser60(B), Leu120(B), Gly121(B), Ser60(A	Tyr119(A), Gln61(A), Tyr59(A), Tyr59(B), Tyr151(B), Tyr119(B), Leu55(D),

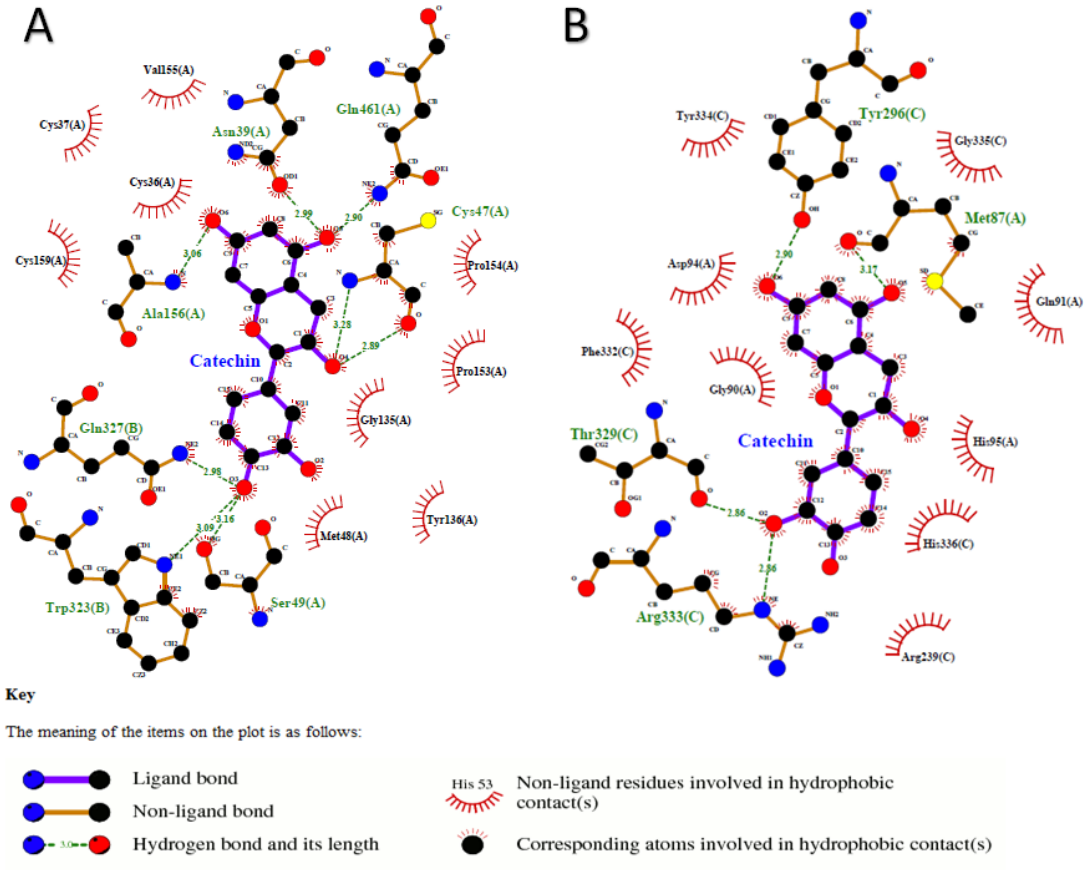


Figure 3. Ligplot+ results for Proteins-ligands complexes. Showing hydrogen bonding with their length (A°), and hydrophobic interactions between catalytic amino acid residues in the active protein target pocket. COX-Catechin complex (A). MPO- Catechin complex (B).

Molecular dynamics simulation study

Catechin, identified as the most promising candidate, underwent molecular dynamics simulation analysis (Figure 4, 5, and 6). The simulation considered the complex formed by catechin with the target proteins COX-2 and MPO. The study employed normal mode mobility analysis, which enabled the examination of B-factors, large-scale mobility, and molecular stability, utilizing the IMOD server. This server facilitated the analysis of internal coordinates based on protein-ligand structural interactions, encompassing B-factor measurement, structural deformation, and eigenvalue calculation. Fig. 4-A and 4-B depict the catechin-bound complexes with COX-2 and MPO. The arrow indicates the direction of motion of amino acid residues. Fig. 4-C and 4-D show the deformability graph for the ligand with COX-2 and MPO, respectively. Peaks in this graph highlight protein regions with deformability. Fig. 4-E and 4-F illustrate the B-factor graph for the catechin complex with COX-2 and MPO, respectively. Main-chain deformability, ligand deformability, and ligand deformation were derived from eigenvalues. These eigenvalues, representing rigidity of motion, are proportional to the energy needed for structural deformation, with lower values indicating simpler deformation. The eigenvalues for our docked complex were 6.652117e-06 for COX-2 and 6.114134e-05 for MPO. Fig. 5-C and 5-D display the variance plot, showcasing individual variances in red and cumulative variance in green. Fig. 6-A and 6-B illustrate the covariance map, indicating motion correlations between residue pairs in red, uncorrelated motion in white, and anti-correlated motion in blue. Fig. 5-C and 5-D depict the elastic map of our docked complex, with dots representing springs between atom pairs, colored based on stiffness (darker grey for stiffer springs, lighter grey for softer springs). The results from the molecular dynamics study revealed a significant degree of deformability in our complex, accompanied by a moderately low eigenvalue, indicating ease of deformation. Notably, the variance map displayed higher cumulative variances compared to individual variances, and

the elastic network map yielded satisfactory outcomes.

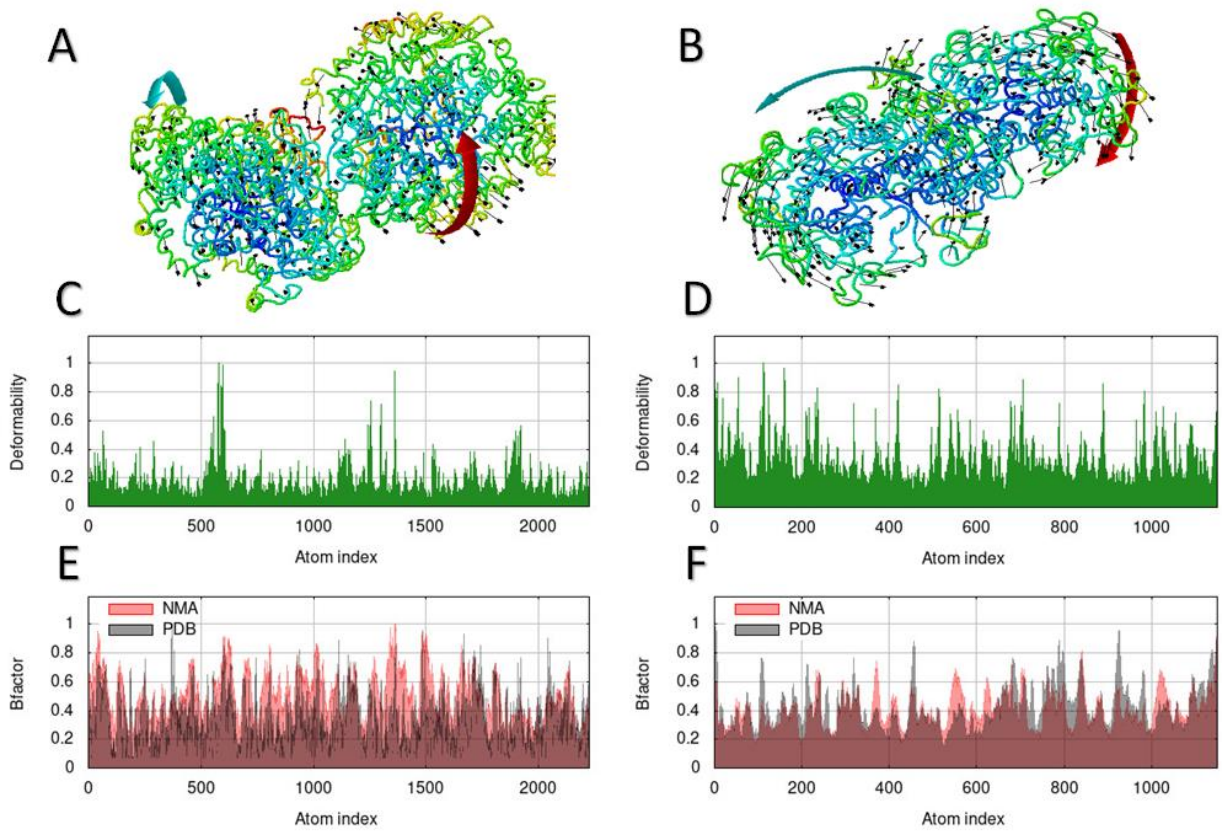


Figure 4. Normal mode analysis (NMA) of the catechin complex with targeted COX-2 and MPO receptors respectively. 3D structure of the interaction (A and B), deformability (C and D), and B factor (E and F).

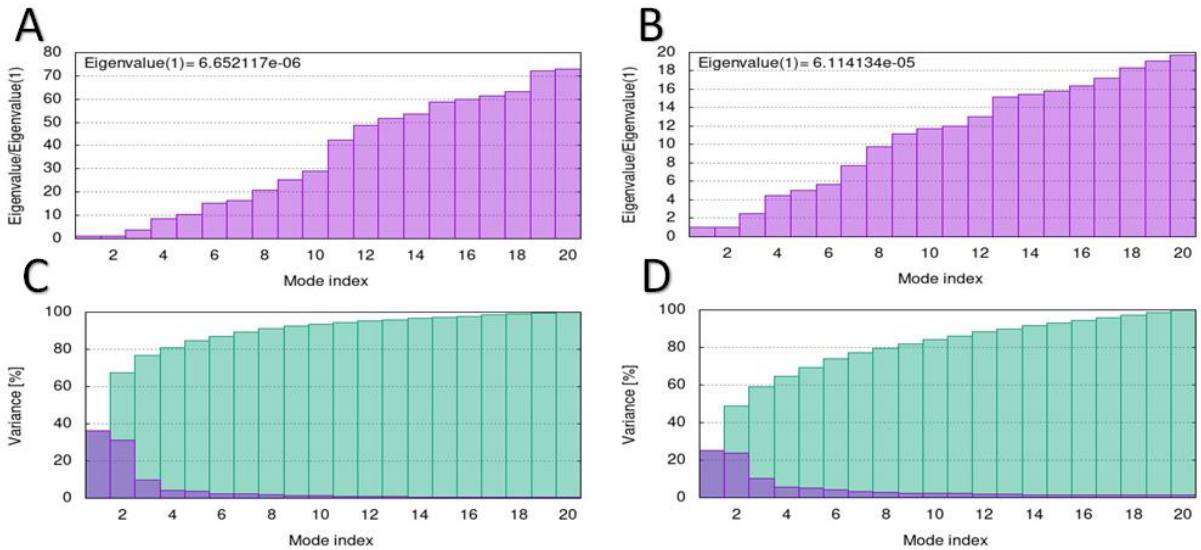


Figure 5. Normal mode analysis (NMA) of the catechin complex with targeted COX-2 and MPO receptors respectively. Eigenvalue (A and B), and variance map (C and D).

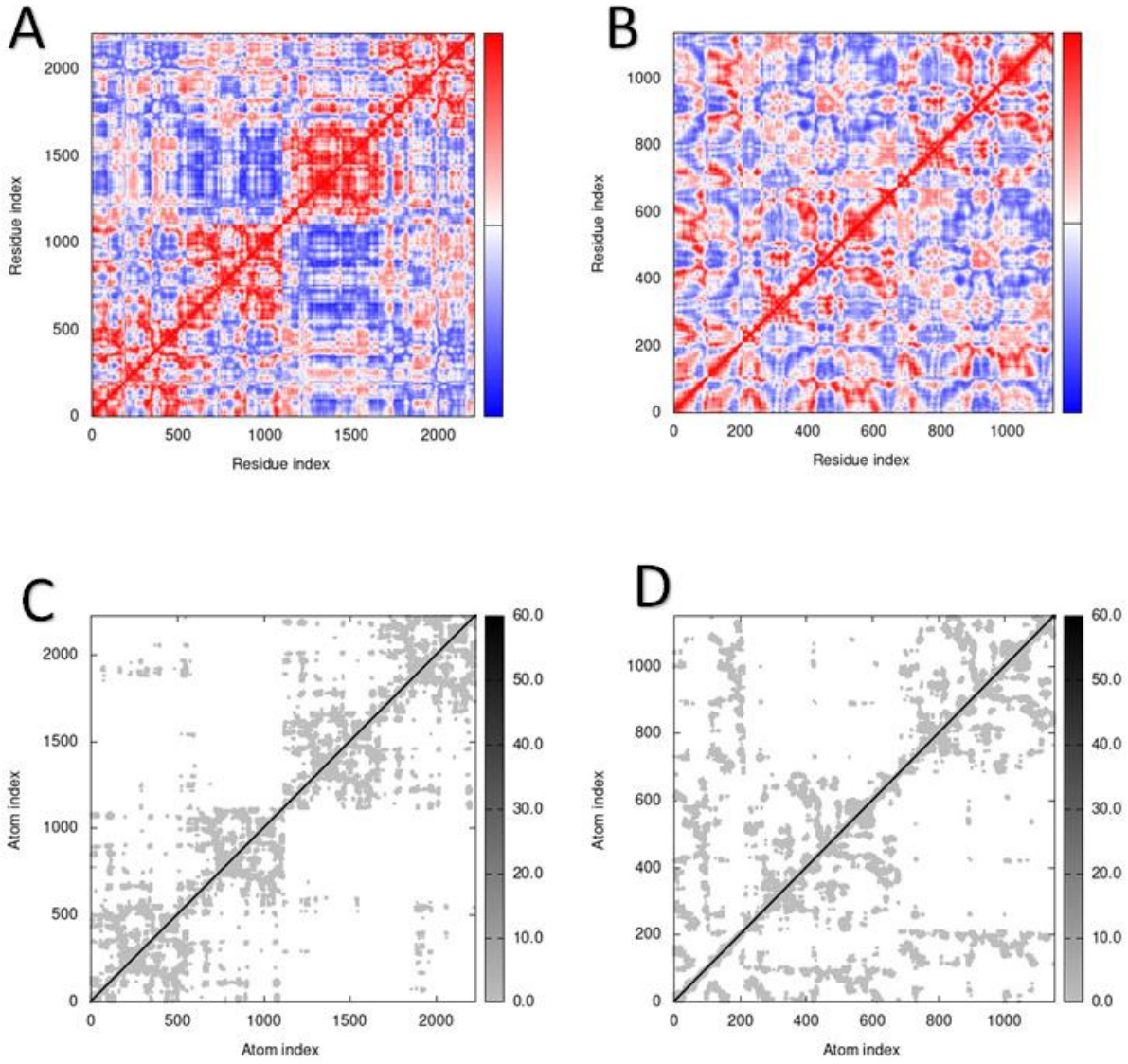


Figure 6. Normal mode analysis (NMA) of the catechin complex with targeted COX-2 and MPO receptors respectively. Correlation matrix (A and B), elastic network model (C and D).

Conclusions

This multidimensional investigation underscores the potential of *Anvillea radiata*-derived phytochemicals, particularly catechin, as promising candidates for the development of novel therapeutics. The prevalence of catechin as a major component in the aqueous extract, coupled with its favorable drug-likeness and low toxicity risks, positions it as a compelling option for further exploration. The observed interactions with crucial target proteins in the molecular docking analysis emphasize its potential therapeutic effects, particularly in the domains of anti-inflammatory. The molecular dynamics simulations provide further evidence of catechin's suitability for drug development, supported by the cumulative variance findings and elastic network map results. Future research, including in silico studies, holds the key to uncovering the underlying mechanisms of these interactions and unlocking the full potential of *A. radiata* phytochemicals for novel drug development.

Declaration of Competing Interest

The authors declare that they have no known competing financial interests or personal relationships that could have appeared to influence the work reported in this paper.

References

1. **Chen, L., Deng, H., Cui, H., Fang, J., Zuo, Z., Deng, J., & Zhao, L.** (2018). Inflammatory responses and inflammation-associated diseases in organs. Oncotarget, 9(6): p. 7204 https://doi.org/10.18632/oncotarget.23208
2. **Weissman, S., Sinh, P., Mehta, T. I., Thaker, R. K., Derman, A., Heiberger, C., & Tabibian, J. H.** (2020). Atherosclerotic cardiovascular disease in inflammatory bowel disease: The role of chronic inflammation. World journal of gastrointestinal pathophysiology, 11(5): p. 104. https://doi.org/10.4291/wjgp.v11.i5.104
3. **Shaikh-Kader, A., Houreld, N. N., Rajendran, N. K., & Abrahamse, H.** (2021). Levels of cyclooxygenase 2, interleukin-6, and tumour necrosis factor-α in fibroblast cell culture models after photobiomodulation at 660 nm. Oxidative Medicine and Cellular Longevity, Volume 2021, p. 13 https://doi.org/10.1155/2021/6667812
4. **Yoshida, N., Ikemoto, S., Narita, K., Sugimura, K., Wada, S., Yasumoto, R., ... & Nakatani, T.** (2002). Interleukin-6, tumour necrosis factor α and interleukin-1β in patients with renal cell carcinoma. British journal of cancer, 86(9): p. 1396-1400. https://doi.org/10.1038/sj.bjc.6600257
5. **Zeinali, M., Rezaee, S. A., & Hosseinzadeh, H.** (2017). An overview on immunoregulatory and anti-inflammatory properties of chrysin and flavonoids substances. Biomedicine & Pharmacotherapy, 92: p. 998-1009. https://doi.org/10.1016/j.biopha.2017.06.003
6. **Ricciotti, E., & FitzGerald, G. A.** (2011). Prostaglandins and inflammation. Arteriosclerosis, thrombosis, and vascular biology, 31(5): p. 986-1000. https://doi.org/10.1161/ATVBAHA.110.207449
7. **Parker, H., & Winterbourn, C. C.** (2013). Reactive oxidants and myeloperoxidase and their involvement in neutrophil extracellular traps. Frontiers in immunology, 3: p. 424. https://doi.org/10.3389/fimmu.2012.00424
8. **Galozzi, P., Bindoli, S., Doria, A., & Sfriso, P.** (2021). The revisited role of interleukin-1 alpha and beta in autoimmune and inflammatory disorders and in comorbidities. Autoimmunity reviews, 20(4): p. 102785. https://doi.org/10.1016/j.autrev.2021.102785
9. **Aliyu, M., Zohora, F. T., Anka, A. U., Ali, K., Maleknia, S., Saffarioun, M., & Azizi, G.** (2022). Interleukin-6 cytokine: An overview of the immune regulation, immune dysregulation, and therapeutic approach. International Immunopharmacology, 111: p. 109130. https://doi.org/10.1016/j.intimp.2022.109130
10. **Forrester, S. J., Preston, K. J., Cooper, H. A., Boyer, M. J., Escoto, K. M., Poltronetti, A. J., & Eguchi, S.** (2020). Mitochondrial fission mediates endothelial inflammation. Hypertension, 76(1): p. 267-276.https://doi.org/10.1161/HYPERTENSIONAHA.120.14686
11. **Rashighi, M., & Harris, J. E.** (2015). Interfering with the IFN-γ/CXCL10 pathway to develop new targeted treatments for vitiligo. Annals of translational medicine, 3(21). https://doi.org/10.3978/j.issn.2305-5839.2015.11.36
12. **Kim, S. J., Flach, A. J., & Jampol, L. M.** (2010). Nonsteroidal anti-inflammatory drugs in ophthalmology. Survey of ophthalmology, 2010. 55(2): p. 108-133. https://doi.org/10.1016/j.survophthal.2009.07.005
13. **Bindu, S., Mazumder, S., & Bandyopadhyay, U.** (2020). Non-steroidal anti-inflammatory drugs (NSAIDs) and organ damage: A current perspective. Biochemical pharmacology, 180: p. 114147. https://doi.org/10.1016/j.bcp.2020.114147
14. **Mahesh, G., Anil Kumar, K., & Reddanna, P.** (2021). Overview on the discovery and development of anti-inflammatory drugs: should the focus be on synthesis or degradation of PGE2? Journal of Inflammation Research, p. 253-263. https://doi.org/10.2147/JIR.S278514
15. **Ng, S. C., & Chan, F. K.** (2010). NSAID-induced gastrointestinal and cardiovascular injury. Current opinion in gastroenterology, 26(6): p. 611-617. https://doi.org/10.1097/MOG.0b013e32833e91eb
16. **Vonkeman, H. E., & van de Laar, M. A.** (2010). Nonsteroidal anti-inflammatory drugs: adverse effects and their prevention. in Seminars in arthritis and rheumatism, 39 (4): p. 294-312 https://doi.org/10.1016/j.semarthrit.2008.08.001
17. **Oray, M., Abu Samra, K., Ebrahimiadib, N., Meese, H., & Foster, C. S.** (2016). Long-term side effects of glucocorticoids. Expert opinion on drug safety, 2016. 15(4): p. 457-465. https://doi.org/10.1517/14740338.2016.1140743
18. **Pribowo, A., Girish, J., Gustiananda, M., Nandhira, R. G., & Hartrianti, P.** (2021). Potential of Tamanu (Calophyllum inophyllum) Oil for Atopic Dermatitis Treatment. Evidence-Based Complementary and Alternative Medicine, volume 2021. p. 9 https://doi.org/10.1155/2021/6332867
19. **Nunes, C. D. R., Barreto Arantes, M., Menezes de Faria Pereira, S., Leandro da Cruz, L., de Souza Passos, M., Pereira de Moraes, L., ... & Barros de Oliveira, D.** (2020). Plants as sources of anti-inflammatory agents. Molecules, 25(16), 3726. https://doi.org/10.3390/molecules25163726
20. **Oguntibeju, O. O.** (2018). Medicinal plants with anti-inflammatory activities from selected countries and regions of Africa. Journal of inflammation research, p. 307-317. https://doi.org/10.2147/JIR.S167789
21. **Miara, M. D., Teixidor-Toneu, I., Sahnoun, T., Bendif, H., & Hammou, M. A.** (2019). Herbal remedies and traditional knowledge of the Tuareg community in the region of Illizi (Algerian Sahara). Journal of arid environments, 167: p. 65-73. https://doi.org/10.1016/j.jaridenv.2019.04.020
22. **Mahdjar, S., Bakka, C., Dendougui, H., & Hadjadj, M.** (2020). Phytochemical profile and In vitro Anti-inflammatory Activity of Anvillea radiata (Coss and Dur) flowers Extracts. Asian Journal of Research in Chemistry, 13(1): p. 44-47. https://doi.org/10.5958/0974-4150.2020.00010.3
23. **Kandouli, C., Cassien, M., Mercier, A., Delehedde, C., Ricquebourg, E., Stocker, P., ... & Pietri, S.** (2017). Antidiabetic, antioxidant and anti inflammatory properties of water and n-butanol soluble extracts from Saharian Anvillea radiata in high-fat-diet fed mice. Journal of ethnopharmacology, 207: p. 251-267. https://doi.org/10.1016/j.jep.2017.06.042

24. **Sharma, D., Chaubey, P., & Suvarna, V.** (2021). Role of natural products in alleviation of rheumatoid arthritis—A review. Journal of food biochemistry, 45(4): p. e13673. https://doi.org/10.1111/jfbc.13673
25. **Serairi-Beji, R., Aidi Wannes, W., Hamdi, A., Tej, R., Ksouri, R., Saidani-Tounsi, M., ... & Karray-Bouraoui, N.** (2018). Antioxidant and hepatoprotective effects of Asparagus albus leaves in carbon tetrachloride-induced liver injury rats. Journal of Food Biochemistry, 42(1): p. e12433. https://doi.org/10.1111/jfbc.12433
26. **Nagavekar, N., & Singhal, R. S.** (2018). Singhal, Enhanced extraction of oleoresin from Piper nigrum by supercritical carbon dioxide using ethanol as a co-solvent and its bioactivity profile. Journal of Food Process Engineering, 41(1): p. e12670. https://doi.org/10.1111/jfpe.12670
27. **Lipinski, C. A., Lombardo, F., Dominy, B. W., & Feeney, P. J.** (2012). Experimental and computational approaches to estimate solubility and permeability in drug discovery and development settings. Advanced drug delivery reviews, 23(1-3): p. 3-25. https://doi.org/10.1016/j.addr.2012.09.019
28. **Ghose, A. K., Viswanadhan, V. N., & Wendoloski, J. J.** (1999). Wendoloski, A knowledge-based approach in designing combinatorial or medicinal chemistry libraries for drug discovery. 1. A qualitative and quantitative characterization of known drug databases. Journal of combinatorial chemistry, 1(1): p. 55-68. https://doi.org/10.1021/cc9800071
29. **Chandra, S., Chatterjee, P., Dey, P., & Bhattacharya, S.** (2012). Evaluation of in vitro anti-inflammatory activity of coffee against the denaturation of protein. Asian Pacific Journal of Tropical Biomedicine, 2012. 2(1): p. S178-S180. https://doi.org/10.1016/S2221-1691(12)60154-3
30. **Azad, I., Nasibullah, M., Khan, T., Hassan, F., & Akhter, Y.** (2018). Exploring the novel heterocyclic derivatives as lead molecules for design and development of potent anticancer agents. Journal of Molecular Graphics and Modelling, 81: p. 211-228. https://doi.org/10.1016/j.jmgm.2018.02.013
31. **Trott, O., & Olson, A. J.** (2010). AutoDock Vina: improving the speed and accuracy of docking with a new scoring function, efficient optimization, and multithreading. Journal of computational chemistry, 31(2): p. 455-461. https://doi.org/10.1002/jcc.21334
32. **Trott, O., & Olson, A. J.** (2010). CASTp 3.0: computed atlas of surface topography of proteins. Nucleic acids research, 46(W1): p. W363-W367. https://doi.org/10.1002/jcc.21334
33. **Dundas, J., Ouyang, Z., Tseng, J., Binkowski, A., Turpaz, Y., & Liang, J.** (2006). CASTp: computed atlas of surface topography of proteins with structural and topographical mapping of functionally annotated residues. Nucleic acids research, 34(suppl_2): p. W116-W118. https://doi.org/10.1093/nar/gkl282
34. **López-Blanco, J. R., Aliaga, J. I., Quintana-Ortí, E. S., & Chacón, P.** (2014). iMODS: internal coordinates normal mode analysis server. Nucleic acids research, 42(W1): p. W271-W276. https://doi.org/10.1093/nar/gku339
35. **Bessada, S. M., Barreira, J. C., & Oliveira, M. B. P.** (2015). Oliveira, Asteraceae species with most prominent bioactivity and their potential applications: A review. Industrial Crops and Products, 76: p. 604-615. https://doi.org/10.1016/j.indcrop.2015.07.073
36. **Chen, L., Chen, N., He, Q., Sun, Q., Gao, M. R., & Zeng, W. C.** (2022). Effects of different phenolic compounds on the interfacial behaviour of casein and the action mechanism. Food Research International, 2022. 162: p. 112110. https://doi.org/10.1016/j.foodres.2022.112110